



El Niño–Southern Oscillation and Pacific Decadal Oscillation impacts on precipitation in the southern and central United States: Evaluation of spatial distribution and predictions

Daniel Kurtzman^{1,2} and Bridget R. Scanlon¹

Received 3 January 2007; revised 18 May 2007; accepted 30 July 2007; published 24 October 2007.

[1] Understanding and predicting regional impacts of El Niño–Southern Oscillation (ENSO) and Pacific Decadal Oscillation (PDO) on winter (October–March) precipitation can provide valuable inputs to agricultural and water resources managers. Effects of ENSO and PDO on winter precipitation were assessed in 165 climate divisions throughout the southern United States. A continuous region of significantly ($P < 0.05$) increased (decreased) winter precipitation in response to El Niño (La Niña) conditions in the preceding summer (June–September Southern Oscillation Index (SOI)) extends across the entire southern United States and as far north as South Dakota. Within this region stronger correlations ($r \leq -0.45$) are found along the Gulf of Mexico, southern Arizona, and central Nebraska. Winter precipitation differs significantly ($P < 0.1$) between warm and cold phase PDO periods only in the south central region, with greatest significance centered in Oklahoma. Enhanced negative La Niña anomalies during PDO cold phases are dominant in the central region (Texas to South Dakota) whereas enhanced positive El Niño anomalies during PDO warm phases are dominant in the southwest (Arizona, Nevada, and California) and southeast (Louisiana to Florida). Validation tests of winter precipitation predictions based on summer SOI and/or PDO-phase show a decrease of 9% to 16% in the relative Mean Absolute Error (MAE) from the MAE obtained by using the mean as a predictor in areas with strong correlation ($r < -0.45$) between SOI and precipitation. Logistic regression probability models of having above or below average winter precipitation had up to 77% successful predictions. The advantage of having probabilities of exceeding certain precipitation thresholds at the beginning of a hydrologic year makes logistic regression models attractive for decision makers.

Citation: Kurtzman, D., and B. R. Scanlon (2007), El Niño–Southern Oscillation and Pacific Decadal Oscillation impacts on precipitation in the southern and central United States: Evaluation of spatial distribution and predictions, *Water Resour. Res.*, 43, W10427, doi:10.1029/2007WR005863.

1. Introduction

[2] Trends in availability of water resources throughout the southern United States are known to be influenced by global atmospheric pressure cycles related to variations in sea surface temperatures (SST). The following provides a brief overview of impacts of two major oceanic/atmospheric cycles on precipitation and water resources in the southern United States.

1.1. Hydrological Impacts of ENSO Based on Large-Scale Studies

[3] El Niño–Southern Oscillation (ENSO) refers to positive (negative) anomalies in SST of the central and eastern equatorial Pacific–El Niño (La Niña), associated with anomalies in equatorial-Pacific sea level pressure (SLP)

differences known as the Southern Oscillation [Rasmusson and Carpenter, 1982; Trenberth, 1997]. The Southern Oscillation Index (SOI), defined as the monthly standardized anomaly of the SLP difference between Tahiti and Darwin, Australia, is a frequently used index of ENSO conditions. A recent review of world-wide environmental and socioeconomic impacts of ENSO indicates that many impacts are related to precipitation, e.g., floods, droughts, spread of water-borne diseases, and agricultural yield [McPhaden *et al.*, 2006].

[4] The following studies used the first harmonic of the composite of 24 months centered in ENSO years (index 0) to delineate regions having a similar hydrologic response time phase (coherence). This method was first introduced by Ropelewski and Halpert [1986]. Four regions were defined as having a coherent precipitation response to ENSO in the United States based on analysis of 1875–1980 data: Gulf of Mexico (GM -Texas to Florida), High Plains (HP), Mid-Atlantic, and Great Basins (GB) [Ropelewski and Halpert, 1986]. The “season” of response was October⁰–March⁺ for the GM region and April⁰–October⁰ for the HP and GB regions (the index + was assigned to months starting in January of the year following the ENSO year). ENSO

¹Bureau of Economic Geology, Jackson School of Geosciences, University of Texas at Austin, Austin, Texas, USA.

²Now at Department of Environmental Health Sciences, Hadassah College, Jerusalem, Israel.

impacts on streamflow were identified in five regions in the United States including the GM and the southwest (SW) based on analysis of 1948–1988 data [Kahya and Dracup, 1993]. A season of increased streamflow corresponding to El Niño events in December⁰ through April⁺ was identified for the GM and in March⁺–November⁺ for the SW (southern California, southern Arizona, and southwest New Mexico). Lower streamflow occurred in response to La Niña from December⁰–August⁺ in the GM whereas streamflow was not sensitive to La Niña in the SW [Dracup and Kahya, 1994]. Regions with coherent responses of the Palmer Drought Severity Index (PDSI) to ENSO included two subregions in the GM: a western (~Texas–GM1) and eastern (~Florida–GM2) region based on analysis of 1900–1993 data [Piechota and Dracup, 1996]. The PDSI in Texas had a significant ($P < 0.1$) positive response (wet conditions) to El Niño in December⁰–August⁺ and a significant ($P < 0.1$) negative response (dry conditions) to La Niña in November⁰–December⁺ whereas the Florida region only had a significant ($P < 0.1$) positive response to El Niño in January⁺–April⁺. PDSI had no significant ($P < 0.1$) response to ENSO in the SW or in the central United States (Kansas, Colorado, and Nebraska).

[5] Teleconnections between ENSO and global precipitation were evaluated using statistical t tests for precipitation composites of El Niño and La Niña extreme events from 1877 to 1982 [Kiladis and Diaz, 1989]. Regions where the P value of t was ≤ 0.05 for a number of adjacent stations were delineated as having a coherent response. El Niño precipitation significantly exceeded La Niña precipitation in a region extending from the Atlantic coast of Florida to the Pacific coast of northern Mexico (including inland Texas) from December⁰–February⁺, this signal persisted through March⁺–May⁺ in south central United States. The full range of an ENSO index (including normal or non-ENSO years) was used to evaluate teleconnections with precipitation in the western United States by Redmond and Koch [1991]. Highly significant ($P < 0.001$) negative correlations between October⁰–March⁺ precipitation and June⁰–November⁰ averaged SOI were found in climate divisions in the SW (New Mexico to southern California), based on analysis of 84 climate divisions in the western United States between 1933 and 1983 [Redmond and Koch, 1991].

1.2. Hydrological Impacts of PDO Based on Large-Scale Studies

[6] Decadal climatic variability driven by SST anomalies in the northern Pacific was termed Pacific Decadal Oscillation (PDO) [Mantua *et al.*, 1997]. PDO is distinguished by warm and cold phases, i.e., decadal scale periods when the SST in the northern Pacific near the North American coast is warmer than average (warm phase) or cooler than average (cold phase). Mantua *et al.* [1997] defined the following PDO phases for the twentieth century: <1925 cold phase; 1925 to 1946 warm phase; 1947 to 1976 cold phase; and >1977 warm phase. There is some confusion about whether a regime shift (back to cold phase) occurred after 1998 [Bond *et al.*, 2003]. Newman *et al.* [2003] claim that ENSO and equatorial SST anomalies are the forcing for the northern SST anomalies and that the PDO index can be predicted with a simple linear model of previous PDO and current ENSO indices. Low correlations ($|r| < 0.25$) between monthly PDO index and winter precipitation were

described by Mantua *et al.* [1997] for the southern United States (data 1990–1993). The PDO cycle modulates ENSO teleconnections, resulting in a stronger El Niño precipitation signal during PDO warm phases and a stronger La Niña signal during PDO cold phases [Gershunov and Barnett, 1998]. There is a “dipole” in precipitation related to multi-decadal ENSO variability in the western United States; i.e., in the PDO cold phase winter precipitation in the SW has a lower correlation with average September–November SOI while winter precipitation in the NW has a higher correlation, the opposite is true for the PDO warm phase [Dettinger *et al.*, 1998; Brown and Comrie, 2004].

1.3. Hydrological Impacts of ENSO and PDO Based on Small-Scale Studies

[7] Many studies have been conducted at the scale of individual states or basins. Andrade and Sellers [1988] showed greatest correlation between El Niño and spring and autumn precipitation, no correlation with summer precipitation of the El Niño year and weaker correlation with the following winter precipitation in Arizona and western New Mexico. Simpson and Colodner [1999], ignoring the emerging PDO-ENSO modulation concept, found a generally decreasing correlation between June⁰–November⁰ SOI and September⁰–April⁺ precipitation excluding January⁺ throughout the twentieth century and relatively large regression slopes between 1924–1946 (PDO warm phase) for one climate division in Arizona. Gutzler *et al.* [2002] found that the annual PDO index did not improve ENSO index predictions of precipitation in climate divisions in Arizona and New Mexico. However, knowledge of PDO phase, rather than PDO index, makes ENSO data more valuable: during PDO cold phase, fall La Niña conditions are generally followed by a dry winter but to lesser extent El Niño conditions are followed by a wet winter; during PDO warm phase, wet El Niño winters are highly probable but not dry La Niña winters. Goodrich [2004] examined non-ENSO years with respect to PDO phase in Arizona and found that winters of PDO cold/non-ENSO years are nearly as dry as winters of PDO cold/La Niña years. Guan *et al.* [2005] showed that PDO phase had a stronger effect than SOI on winter precipitation in the mountainous region of northern New Mexico. Namely non-ENSO and even La Niña years during PDO warm phase had significant positive anomalies while El Niño years during PDO cold phase did not have a positive anomaly.

[8] Hanson *et al.* [2004] applied frequency analysis to data from the Mojave River Basin, California, and showed that PDO range (10–25 annums (a)) reconstructed components (frequencies) captured 83% of streamflow variance and 75% of groundwater level variance. In contrast, ENSO related frequencies (2–6 a) captured only 7–12% of streamflow and 17% of groundwater level variances. Pool [2005] showed greater probability of above average winter precipitation, streamflow, and groundwater recharge during El Niño years and almost exclusively below average conditions during La Niña years in southern Arizona. Sun and Furbish [1997] reported that ENSO was responsible for up to 40% of annual precipitation variation and up to 30% of river discharge variation in Florida. El Niño years were wetter than average and La Niña years were drier. These authors used annual precipitation rather than seasonal precipitation, which was used in most of the aforementioned

studies. Annual stream discharge was also used by *Redmond and Koch* [1991]. Correlations between ENSO indices and stream discharge in Florida and the SW are similar ($r \sim 0.3-0.4$) in these two studies [*Sun and Furbish*, 1997; *Redmond and Koch*, 1991]. *Chen et al.* [2005] evaluated the ENSO-dependent component of water and agricultural management of the Edwards aquifer in Texas (1970–1996 data). They concluded that use of ENSO events has the potential to help offset costs of diminishing regional pumping due to legislative mandates.

1.4. Approach and Objectives

[9] Previous studies vary in the spatial scale evaluated (global to state/basin level), time period considered (27 to >100 a), ENSO index used (SOI, SST indices), analysis approach (harmonics, t tests, correlations, or frequency analysis), seasons of forcing and response, and whether PDO phases were considered. The time period considered in hydro-climatology studies is important because it determines the number of PDO cold and warm phase years included in the analysis. Dominance of one phase (e.g., 1970–2000, dominated by PDO warm phase) may bias results; therefore, a period including an equal number of years of PDO cold and warm phases was used in this study. Many small scale studies focused on ENSO and/or PDO impacts on precipitation in the SW United States rather than in the south central and SE United States, although some phenomena are stronger in the latter areas. Results from global analyses may differ from those of local analysis because of differences in spatial resolution, as exemplified by differing results for southern Brazil provided by global analysis [*Ropelewski and Halpert*, 1987] and by a local analysis [*Grimm et al.*, 1998]. Therefore, a statistical descriptive analysis of ENSO and PDO impacts on winter precipitation throughout the entire southern United States at a climate-division resolution can provide an improved regional perspective, which is lacking in both global/continental and state/basin scale studies. Previous studies have not explicitly tested the validity of simple statistical precipitation predictions based on ENSO/PDO data, especially the use of logistic regression models, for quantifying probabilities of exceeding precipitation thresholds; however, such analyses can be extremely beneficial to agricultural and water-resource managers.

[10] These issues helped define the research objectives of this study to address the following questions: (1) What is the extent of the region throughout the southern United States where a significant precipitation response to ENSO exists, i.e., wetter than normal winters following El Niño summers? (2) What are the spatial distribution and relative importance of ENSO, PDO, and combined ENSO and PDO on winter and annual precipitation in the region defined in 1? (3) What is the validity of predictions of winter precipitation based on simple statistical models, such as linear and logistic regressions, using ENSO and/or PDO in representative areas of the region defined in 1?

2. Methods

2.1. Precipitation Data and Climatic Variables Selection

[11] A variety of indices are available to represent ENSO conditions based on SST (e.g., Nino-3, Nino-4, Nino-3.4 and

Japan Meteorological Agency, JMA index), sea level pressure (e.g., SOI) and combinations of different oceanic and atmospheric variables (e.g., Multivariate ENSO Index, MEI [*Wolter and Timlin*, 1993]). SOI was chosen in this study because it is publicly available in real time (i.e., September SOI is available on 2 October), it has the longest period of record (1876 to present), and it was successfully used in previous climate analyses of different areas in the southern United States [e.g., *Redmond and Koch*, 1991; *Piechota and Dracup*, 1996; *Pool*, 2005]. Monthly SOI values were obtained from the Australian Bureau of Meteorology (<http://www.bom.gov.au/climate/glossary/soi.shtml>). The June–September average of monthly SOI was used in this study to provide an ENSO index that would be available at the beginning of the hydrologic year (1 October [*Chen et al.*, 2005]). The June–September average of monthly SOI is similar to the June–November average ($r^2 = 0.95$) that was successfully used in previous studies [e.g., *Redmond and Koch*, 1991; *McCabe and Dettinger*, 1999]. For the 100 years 1905–2004, 9 out of the 10, and 23 out of the 25 strongest El Niño years (negative SOI) are the same for both indices (June–September and June–November SOI averages) and similarly for the strongest La Niña years (i.e., 9 out of 10 and 23 out of 25).

[12] Monthly PDO indices, defined as the leading principle component (PC1) of monthly SST anomalies in the North Pacific Ocean, pole-ward of 20°N, were obtained for the period 1900 to 2005 (Joint Institute for the Study of the Atmosphere and Ocean, JISAO; <http://jisao.washington.edu/pdo/PDO.latest>). Following *Gutzler et al.* [2002], rather than using the PDO index, discrete PDO phases were revealed from 9 a moving averages of annual and November–March PDO indices (Figure 1). The November–March mean was used to delineate PDO phases by *Mantua et al.* [1997] and *Hidalgo and Dracup* [2003]. A 9 a window was chosen because it clearly reveals the multi-decadal frequency and yet it is not too long. Moving averages of the June–November SOI index were plotted together with the PDO indices to define the decadal phase changes because *Newman et al.* [2003] showed a clear linkage between Pacific equatorial SST (ENSO) and northern Pacific SST (PDO) anomalies. *Hanley et al.* [2003] also showed correspondence between running sums of ENSO indices and PDO-phase changes. The PDO moving average analysis (Figure 1) suggests the following PDO phases: warm 1922–1944, cold 1945–1977, and warm 1978–2004. The two PDO moving average series for 1905–1921 have low amplitudes and change from positive to negative around 1912, whereas the SOI series shows a more consistent cold pattern (Figure 1); therefore, this period (1905–1921) was assigned to a cold phase. The century (1905–2004) includes 50 PDO cold phase and 50 PDO warm phase years; therefore, biases resulting from dominance of one phase over another are avoided (Figure 1). In some studies 1998 is defined as the end of the warm phase [e.g., *Peterson and Schwing*, 2003]. Although PDO indices between 1999 and 2002 have mostly negative values, PDO indices between 2003 and 2006 have almost all positive monthly values, making the decadal phase shift still unclear.

[13] The National Climate Data Center (NCDC) averages meteorological data from stations spatially to represent areas defined as climate divisions (see Figure 2 for climate

region of analysis was defined by a threshold correlation significance of $P \leq 0.05$ ($\sim r \leq -0.2$ for the 100 a data) between SOI and winter precipitation. The southern states were examined first and if the northern climate divisions in the state showed significant correlation the neighboring state to the north was examined until the entire continuous WEW region throughout the southern United States was delineated.

[15] Serial correlation in time series can reduce the effective degrees of freedom and therefore reduce the level of statistical significance related to correlation coefficients. *McCabe and Dettinger* [1999] addressed this issue when correlating June–November average SOI with winter precipitation in the western United States, and concluded that their 30 a series of indices could be regarded as independent (0 serial correlation). Serial correlations in SOI used in this study were evaluated in 56 series of 75 a each for correlations between pairs of series lagging from 1 to 10 a. The highest absolute average correlation coefficient was found for the 7 a lag ($\langle r \rangle = 0.18$). No pair of series out of the 505 pairs tested had a correlation coefficient that was statistically different from zero at a confidence level of $P = 0.1$; therefore, the 100 a SOI time series used in this study was treated as independent and correlation significance was calculated with 98 degrees of freedom.

[16] The following analyses were performed for each climate division of the southern WEW continuous region. The correlation coefficient, statistical significance (P value of the regression coefficient), and linear regression model were calculated for winter (October⁰–March⁺) and annual (October⁰–September⁺) precipitation versus SOI. The El Niño and La Niña precipitation anomalies were derived for composites of 10% and 25% SOI-extreme years. T tests for differences in mean precipitation between PDO cold and warm phases were conducted and associated P values were calculated assuming the 50 a of precipitation are serially independent. PDO-50% cold (warm) phase precipitation anomalies were compared with SOI 50% precipitation anomalies (50% higher (lower) SOI years) to delineate areas with a higher PDO or ENSO response. El Niño–PDO warm phase, El Niño–PDO cold phase, La Niña–PDO warm phase, and La Niña–PDO cold phase anomalies for each climate division were calculated to test decadal modulation of ENSO.

2.2.2. Precipitation Predictions and Validation Tests

[17] Two categories of winter-precipitation predictions were examined: (1) continuous predictions, where the exact precipitation amount was predicted; (2) dichotomous predictions, where a prediction of exceeding a certain precipitation threshold was determined. All predictions were tested for six selected climate divisions.

[18] The predictions of eight continuous predictors were compared. Two trivial predictors (i.e., predictors that do not use any SOI or PDO-phase data) were evaluated: the mean and median precipitation of the climate division. The third continuous predictor was the linear regression model of winter precipitation versus SOI (SOI Reg.). The fourth predictor was a three number predictor; i.e., the winter precipitation data were divided into three categories according to the ENSO conditions of the previous June–September: El Niño (25% low SOI), La Niña (25% high SOI) and Non-ENSO (the second and third quartiles of SOI). The mean

precipitation of each of the three categories was the predicted winter precipitation according to the ENSO conditions that preceded the predicted-winter (NNN). In the same manner as the fourth predictor, the fifth predictor was a two number predictor including: average winter precipitation in 50 a PDO warm phase or in 50 a PDO cold phase (PDO). The sixth predictor was a superposition of SOI Reg. and PDO anomaly (SOI Reg. + PDO). The seventh predictor was a choice between two SOI-precipitation linear regression models, one derived from PDO cold phase years and one from PDO warm phase years (Two Reg.). The last predictor was a six number predictor including average winter precipitation for the following conditions: El Niño-PDO warm phase, El Niño-PDO cold phase, La Niña-PDO warm phase, La Niña-PDO cold phase, Non-ENSO-PDO warm phase, and Non-ENSO-PDO cold phase (Six).

[19] Logistic regression models (equation (1)) were used to predict the probability of winter precipitation being above or below the mean and the first quartile. The logistic regression model calculates the probability - Pr for one of two possible outcomes of the dependent variable y using the following equation (in our case: $y_i = 1$ means above the precipitation threshold in year i).

$$\Pr(y_i = 1) = \frac{e^{(\alpha + \beta_1 x_{i1} + \beta_2 x_{i2} + \dots + \beta_k x_{ik})}}{1 + e^{(\alpha + \beta_1 x_{i1} + \beta_2 x_{i2} + \dots + \beta_k x_{ik})}} \quad (1)$$

where $x_1, x_2 \dots x_k$ are explanatory variables (in our case two variables SOI and PDO phase) and α and $\beta_1, \beta_2 \dots \beta_k$ are model coefficients. A stepwise variable-selection method was used in SAS [*SAS Institute Inc.*, 2004] for determining model coefficients, in which only statistically significant explanatory variables were incorporated into the model. This means that either SOI or PDO phase, or both, or neither were used in the logistic model. $\Pr(y_i = 1) > 0.5$ was assigned as above threshold prediction. The percentage of successful predictions was compared to the trivial prediction: “always below the mean” (precipitation distributions are skewed and there is more than 50% probability of having below mean precipitation) and “always above the first quartile” ($\Pr = 75\%$). The level of success of predictions for the subset of years in which the logistic regression models gave high or low probabilities [$\Pr(y_i = 1) > 0.6$ and $\Pr(y_i = 1) < 0.4$] was also evaluated.

[20] The following prediction-validation procedure was used for both continuous and dichotomous predictions. The 100 a of precipitation, SOI, and PDO data were sorted according to precipitation. Five sets of 20 records were taken out for validation by removing records numbered 1-6-11...96, 2-7-12...97, 3-8-13...98, 4-9-14...99 and 5-10-15...100. For each one of these 20 record sets the corresponding set of the remaining 80 records was used for estimating the predictors (i.e., record numbers 2-3-4-5-7-8...-100, 1-3-4-5-6-8...-100, 1-2-4-5-6-7...-100, etc.). In this way prediction models were relatively unbiased, which is the case when using all the available data for real prediction of the following winter precipitation. Another advantage of this method is that each one of the 100 a of precipitation data was predicted once. The Mean Absolute Error (MAE) of the 100 predictions was compared among the eight continuous predictors to determine the best continuous predictor. The percentage of successful predictions

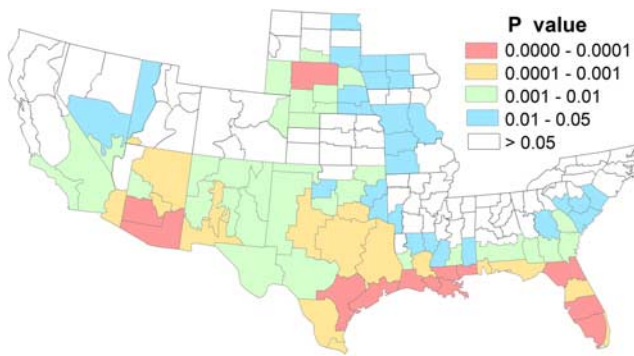


Figure 3. P values for the regression coefficient between June⁰–September⁰ SOI and annual October⁰–September⁺ precipitation in the Wet El Niño Winter (WEW) region in the southern United States.

was examined for dichotomous predictions (logistic regression models). Both MAE and percentage of successful predictions were compared with those obtained from trivial predictors to assess improvement in prediction due to use of SOI and PDO data.

3. Results and Discussion

3.1. Wet El Niño Winter (WEW) Region

[21] A continuous, statistically significant WEW region extends from North Carolina to southern California. Its south-north extent varies from lowest along the Gulf Coast in Mississippi and Alabama to highest from southern Texas to South Dakota (Figure 2). Three areas of higher significance are evident: Gulf of Mexico including most of Texas (GM), southern Arizona and New Mexico (SW), and north central Nebraska (Nebraska) (Figure 2). This WEW region and the three centers differ from the large scale precipitation-ENSO zones defined in previous studies [Ropelewski and Halpert, 1986; Kiladis and Diaz, 1989] by: (1) the coast to coast continuity throughout the southern United States, and (2) the northward extent in the High Plains including the high correlation center in Nebraska. Many of the studies that concentrated on the western United States [e.g., Redmond and Koch, 1991; Brown and Comrie, 2004] did not include Nebraska; therefore, this area had not been delineated as an ENSO affected region previously.

[22] The GM and SW WEW centers can be explained by the southerly shift of storm tracks associated with the Subtropical Jet Stream in El Niño years [Trenberth et al., 1998; Eichler and Higgins, 2006]; however, the Nebraska WEW center cannot be explained by the relative abundance of storm tracks along the Subtropical Jet. A more frequent southward movement of the Polar Jet Stream that converges with the Subtropical Jet in El Niño winters may explain the Nebraska WEW center (e.g., the 24–25 October storm during the strong El Niño year of 1997 described in http://cimss.ssec.wisc.edu/goes/misc/oct97_winter_storm.html [CIMSS, 2006]). Noel and Changnon [1998] examined the correlation between frequency of winter cyclones and ENSO events. They suggested that during El Niño events, where the 28°C SST isotherm near the equator is west of longitude 150°W, the Polar-Jet related cyclones are dis-

placed to the south, resulting in more winter cyclone events in the Nebraska WEW region (Figure 2).

3.2. Annual Precipitation

[23] Correlation between SOI and annual precipitation for the continuous WEW region also includes three hotspots (SW, GM, and Nebraska), similar to those identified for the October⁰–March⁺ precipitation; however, hot spot areas are smaller and P values are higher (significance of correlations is lower) for annual precipitation (Figure 3). Similarity in responses for winter (Figure 2) and annual precipitation (Figure 3) is consistent with results from other studies that identified relationships between ENSO and hydrologic variables in the spring and summer following March⁺ [Dracup and Kahya, 1994; Piechota and Dracup, 1996].

3.3. ENSO and October⁰–March⁺ Precipitation Anomalies

[24] Comparison of relative precipitation anomalies of the 25 strongest El Niño years (SOI ≤ -0.57) and of the 25 strongest La Niña years (SOI ≥ 0.58) shows that positive anomalies in the El Niño composite are larger than negative anomalies in the La Niña composite (notice the larger red and orange areas in Figure 4a relative to those in Figure 4b, similarly for Figures 4c and 4d). This is partly because relative positive precipitation responses to extreme ENSO conditions are not bounded whereas relative negative responses cannot exceed 100%. The Arizona SW climate division (bold boundaries in Figures 4a–4c) has the highest relative positive anomaly in El Niño winters (47% in the upper quartile composite and 75% in the upper decile) as well as the strongest negative anomaly in La Niña winters (-32%) and it is the only climate division that has a negative anomaly stronger than -25% for the upper quartile SOI years composite. The composite of the 10% most extreme El Niños (SOI ≤ -1.36) reveals the entire southwest as the region that is affected most dramatically by extreme El Niño conditions (Figure 4c). This is probably the reason why this area was the subject of many small scale ENSO studies, mentioned previously (section 1.3). The high negative precipitation anomalies for the 10% extreme La Niña conditions (SOI ≥ 1.10) shift eastward relative to the high positive precipitation anomalies for the 10% extreme El Niño conditions, leaving California almost unaffected (Figures 4d and 4c). Texas and the western GM suffer from stronger negative anomalies during extreme La Niña winters than positive anomalies during extreme El Niño winters (Figures 4d and 4c). The combination of the aforementioned differences between the SW and the south central regions and the higher relative variability of precipitation in the SW is another reason for the overall observation that relative positive anomalies after El Niño are stronger than relative negative anomalies after La Niña.

[25] When absolute quantities of precipitation anomalies rather than relative anomalies are considered, the GM region is the region most affected by ENSO rather than the SW or Nebraska (Figure 5). For composites of upper and lower quartiles of SOI, the Southeast Louisiana climate division has the highest winter El Niño anomaly (+128 mm) while the Gulf climate division in Alabama has the strongest winter La Niña anomaly (-100 mm). The highest annual El Niño anomaly (+160 mm) is in the Coastal climate division of Mississippi and the strongest annual La Niña

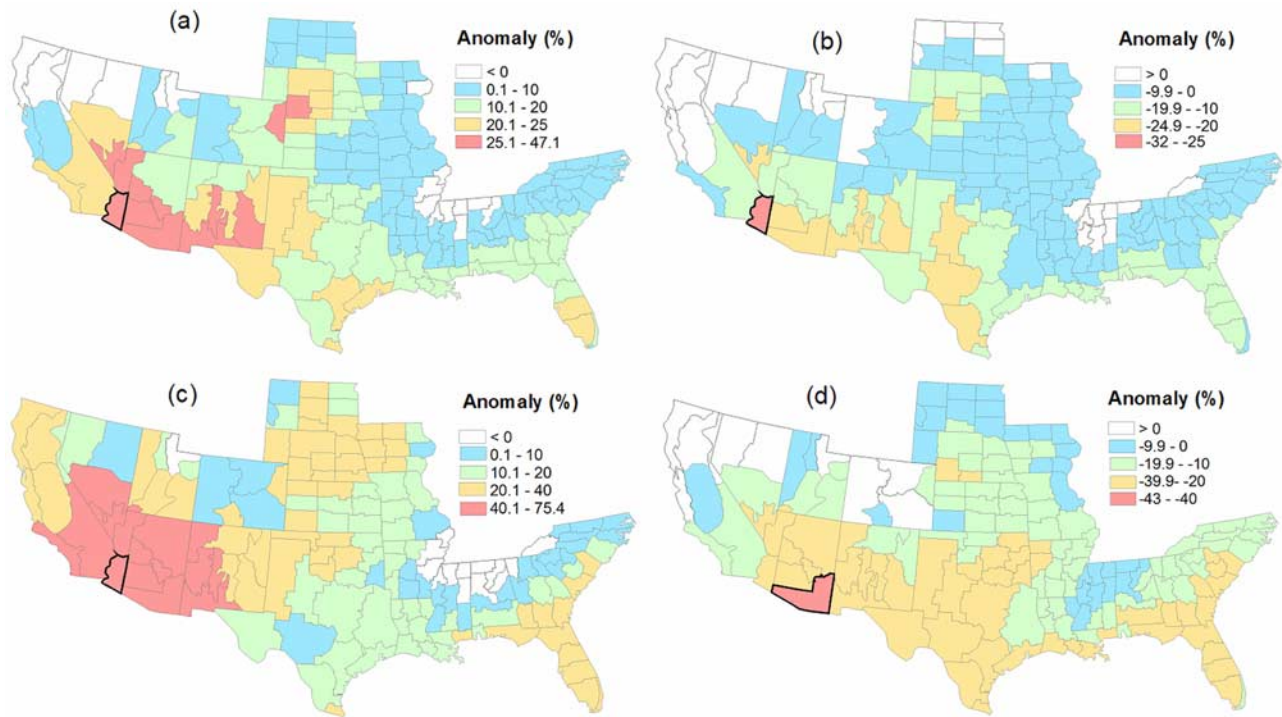


Figure 4. October⁰–March⁺ relative precipitation anomalies (in % of 100 a mean) for (a) the 25% strongest El Niño years, (b) the 25% strongest La Niña years, (c) the 10% strongest El Niño years, and (d) the 10% strongest La Niña years. Climate divisions with the strongest anomalies are in bold.

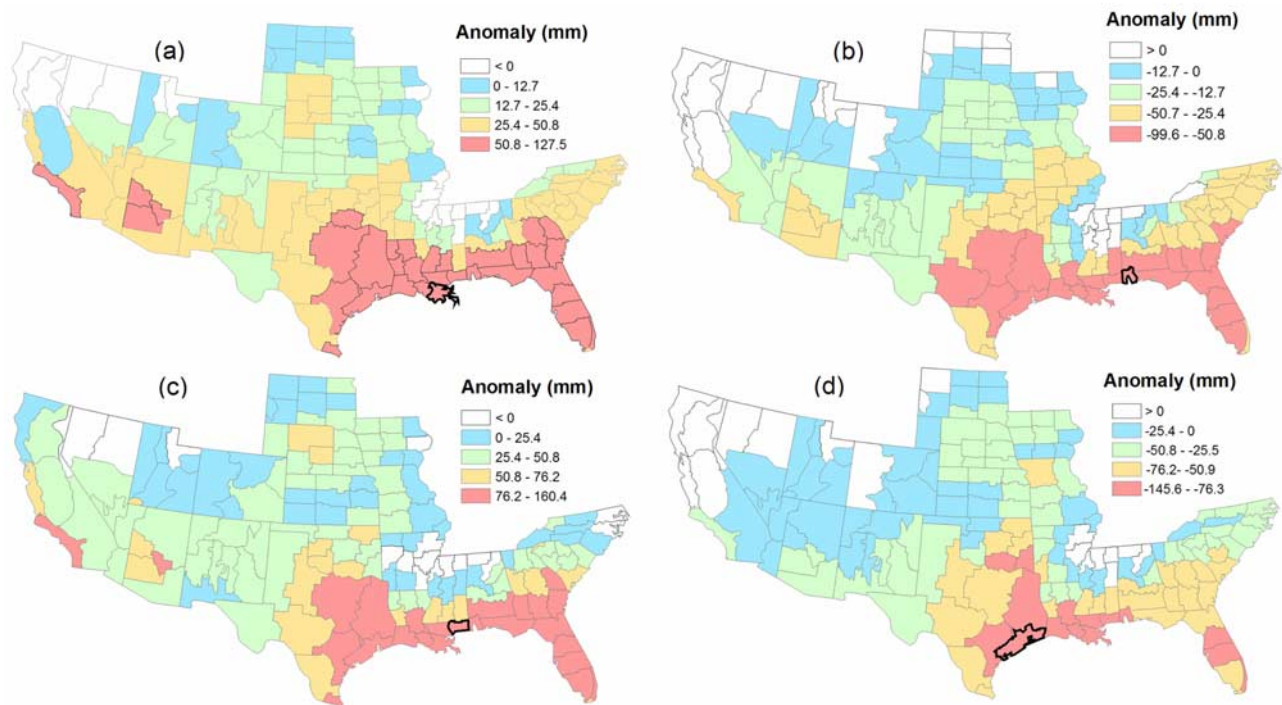


Figure 5. Absolute precipitation anomalies (in mm) for composites of the upper and lower 25% SOI for (a) El Niño year's winter (October⁰–March⁺), (b) La Niña year's winter, (c) El Niño years annual (October⁰–September⁺), and (d) La Niña years annual. Climate divisions with the strongest anomalies are in bold.

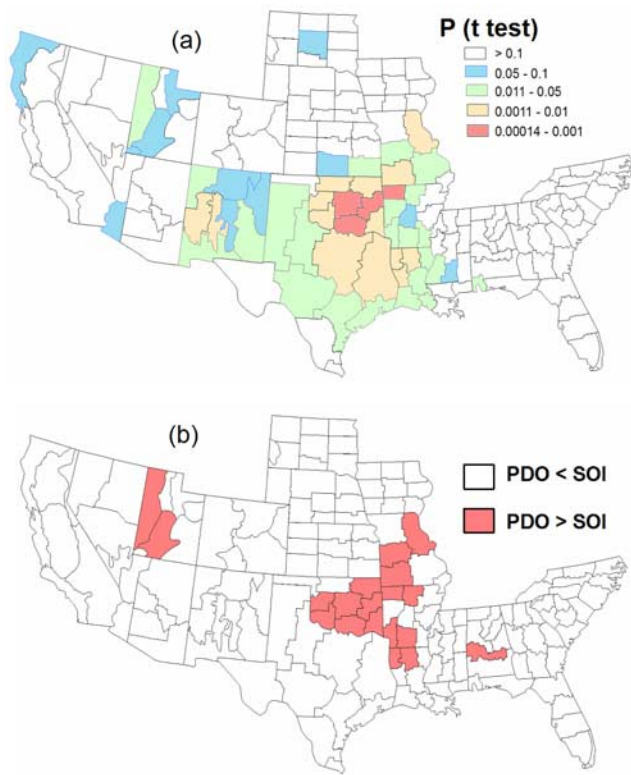


Figure 6. (a) P values for t test of the difference between October⁰–March⁺ precipitation of PDO warm and cold phase composites. (b) Area within the southern WEW region in which the winter (October⁰–March⁺) precipitation anomaly of the 50% composite of PDO warm (cold) phase is greater than the 50% composite of negative (positive) SOI.

anomaly (–146 mm) is in the Texas Upper Coast climate division (boundaries for the aforementioned climate divisions are bolded in Figure 5).

3.4. PDO and Winter Precipitation Anomalies

[26] The effect of PDO phase on October⁰–March⁺ precipitation was analyzed using a t test to determine significance of the difference in the mean of the two 50-a composites of PDO cold (1905–1921, 1945–1977) and PDO warm (1922–1944, 1978–2004) phases (Figure 6a). Winter precipitation is significantly different ($P < 0.1$) between PDO phases in the south central region from New Mexico to Louisiana, with the highest significance (lowest P values) centered in Oklahoma (Figure 6a). Although low correlations between precipitation and PDO index were shown for this area by *Mantua et al.* [1997], the current t test analysis suggests that knowledge of the PDO phase can improve winter precipitation predictions in this region.

[27] Areas where the 50% PDO warm (cold) phase composite winter precipitation anomaly is greater than the 50% SOI winter precipitation anomaly are shown for climate divisions that had significant correlation ($P < 0.05$) between SOI and winter precipitation (Figure 6b). The 50% SOI composites are simply the 50 a, out of the 100 a of data used in this study, in which $SOI > 0$ (the La Niña composite) and the other 50 a where $SOI \leq 0$ (the El Niño

composite). The continuous area where PDO had a greater influence on winter precipitation than the more frequent ENSO cycle is restricted to the central region (Figure 6b) and does not include the three WEW hotspots (SW, GM, and Nebraska). In light of these results, the effect of the many small spatial scale studies that dealt with relationships between PDO and water-resource variables in the SW [e.g., *Hanson et al.*, 2004; *Goodrich*, 2004; *Guan et al.*, 2005] may provide a biased impression of regions in the southern United States where the PDO effect is significant.

3.5. Combined ENSO and PDO Effects

[28] Strengthening El Niño positive anomalies during PDO warm phase (13 a) and reducing this effect during PDO cold phase (12 a) is termed the El Niño Decadal Modulation (ENDM, Figure 7a). Similarly, strengthening La Niña negative anomalies during PDO cold phase (18 a) and reducing this effect during PDO warm phase (7 a) is termed La Niña Decadal Modulation (LNNDM, Figure 7b). While the ENDM exists in the south central part of the study area, it does not exist at all (there is even a negative ENDM) in the north central part (Kansas, Nebraska and South Dakota) (Figure 7a). ENDM is greatest in areas most affected by PDO in the south central region (New Mexico–Louisiana; Figures 6a and 7a); however, ENDM also occurs in the southeast (Florida) and southwest (southern Nevada, Arizona, and California) (Figure 7a). LNNDM is confined to the central region and is negligible in the southeast and southwest (Figure 7b). In contrast to the ENDM, the LNNDM is strong in the Nebraska–South Dakota area. The frequency of La Niña years is also higher during PDO cold phase (36% in PDO cold phase versus 25% in both phases) while the frequency of El Niño years during PDO cold phase is not significantly less than the general frequency. It seems that in the southern United States the PDO modulation is more related to La Niña than to El Niño (compare total red areas between Figures 7a and 7b). Although the Oklahoma, northern Arkansas, and Missouri region is not a high ENSO region, it is within the southern WEW (Figure 2), and it is influenced by PDO phases, particularly during La Niñas (Figures 5b, 6, and 7). There is a sharp divide between the central area where the LNNDM is stronger (orange and red in Figure 7c) than the southwest and southeast regions where the ENDM is dominant (green and blue in Figure 7c).

3.6. Predictions of Winter Precipitation

[29] Six climate divisions were selected to test the predictability of winter (October⁰–March⁺) precipitation (Table 1 and Figure 8a). The WEW centers are represented by TX8 and FL3 (GM), NE2 (Nebraska), and AZ4 (SW) (Figures 2 and 8a). The PDO dominant region is represented by OK8 (Figures 6 and 8a). California division 7 (CA7) was chosen to represent an area with significant, but low, correlation with SOI (Figures 2 and 8).

[30] In all six divisions, knowledge of the June⁰–September⁰ SOI (and the PDO-phase in two out of the six) improved the prediction of winter (October⁰–March⁺) precipitation relative to the mean or median trivial predictors (Table 1 and section 2.2.2 for the different predictors). Relative improvement from the mean prediction [defined as: $(MAE_{\text{mean}} - MAE_{\text{predictor}})/MAE_{\text{mean}}$ expressed in percent] was relatively low (3.7–5.4%) for OK8, CA7, and AZ4, which are characterized by low correlations between SOI

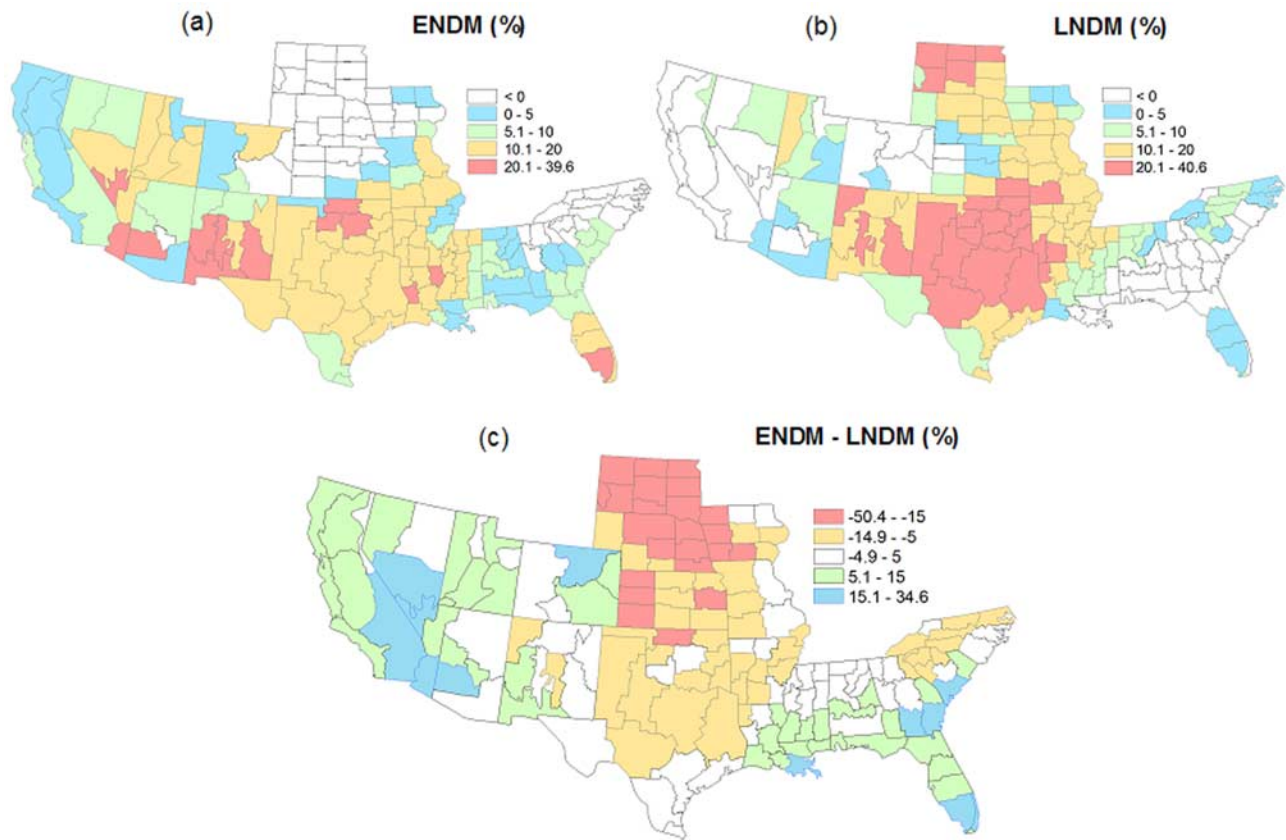


Figure 7. (a) Mean winter (October⁰–March⁺) precipitation of the composite of the lower quartile SOI which occurred during PDO warm phase minus the mean winter precipitation of the composite of the lower quartile SOI which occurred during PDO cold phase – El Niño Decadal Modulation (ENDM). (b) Mean winter (October⁰–March⁺) precipitation of the composite of the upper quartile SOI which occurred during PDO warm phase minus mean precipitation of the composite of upper quartile SOI which occurred during the PDO cold phase – La Niña Decadal Modulation (LNDM). (c) ENDM – LNDM. Scales are in percents of the 100 a winter precipitation mean.

Table 1. Validation Test Results for Predictions of October⁰–March⁺ Precipitation Using June⁰–September⁰ SOI and PDO Phase, and Some Related Statistics of These Variables for Six Representative Climate Divisions

Parameter or Predictor		Climate Division					
		TX8	OK8	FL3	CA7	AZ4	NE2
Statistics	SOI-Precipitation Correlation (r)	-0.52	-0.33	-0.46	-0.30	-0.40	-0.47
	PDO-Precipitation Anomaly ^a (% of mean)	7.2	10.8	1.4	2.2	1.7	4.3
Continuous predictions Mean Absolute Error (MAE) of precipitation predictions (% of mean)	mean (trivial ^b)	23.4	25.8	26.1	40.1	33.9	25.9
	median (trivial)	23.2	25.5	25.9	38.7	33.4	25.8
	Best prediction (lowest MAE)	19.6	24.4	23.4	38.4	32.6	23.5
	Best predictor ^c	SOI Reg. + PDO	SOI Reg. + PDO	SOI Reg.	SOI Reg.	SOI Reg.	SOI Reg.
	Relative improvement from mean, ^d %	16.2	5.4	10.3	4.2	3.7	9.0
Dichotomous predictions Successes of above or below mean precipitation predictions (% of successful predictions)	Always below (trivial)	54	56	53	61	57	52
	Logistic – Pr > 0.5 – above mean, Pr < 0.5 below mean	72	64	67	65	60	67
	Improvement from trivial ^e	18	8	14	4	3	15
	Logistic – Pr < 0.4 or Pr > 0.6 ^f	75	70	77	66	71	76
Above or below first quartile	Logistic – Pr > 0.5 – above, Pr < 0.5 below	81	79	76	75	71	76

^aAbsolute deviation of mean precipitation of the 50% warm (cold) PDO years from the 100 a mean.

^bTrivial predictions refer to predictions that do not use SOI and/or PDO data.

^cSee section 2.2.2, second paragraph for a description of the different predictors.

^d(MAE_{mean} – MAE_{predictor})/MAE_{mean} expressed in percent.

^eDifference in percent of successful predictions between predictions of the Logistic model in the row above and the trivial prediction.

^fSee section 3.6, fifth paragraph for the difference between (Logistic – Pr > 0.5 – above mean, Pr < 0.5 below mean) and (Logistic – Pr < 0.4 or Pr > 0.6).

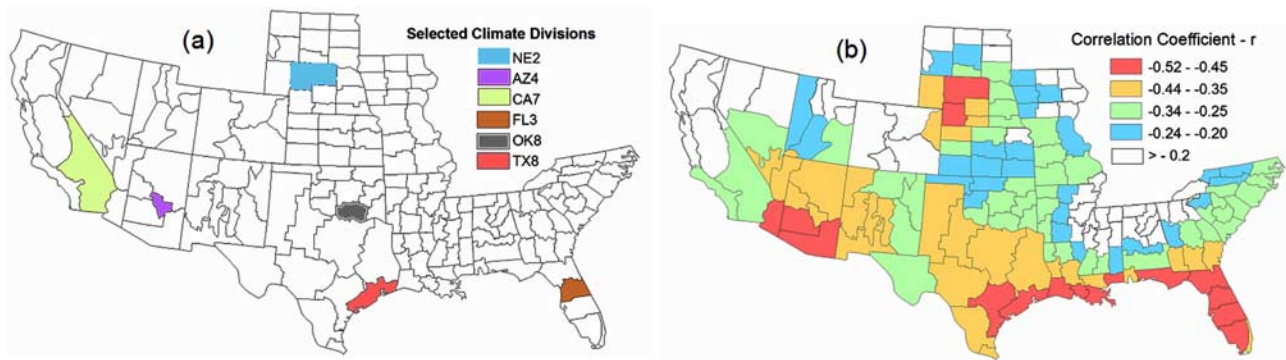


Figure 8. (a) Selected climate divisions where predictability of winter precipitation was tested. (b) Correlation coefficients $-r$ for June⁰-September⁰ SOI and October⁰-March⁺ precipitation. Note areas in red where $r < -0.45$.

and winter precipitation ($r \geq -0.4$, Table 1). In contrast, relative improvement from trivial predictors was much higher (9.0–16.2%) for TX8, FL3, and NE2 climate divisions, which are characterized by higher correlation between SOI and winter precipitation ($r < -0.45$, Table 1).

[31] Regression predictors (e.g., SOI Reg., SOI Reg. + PDO) were superior to fixed number predictors in all six climate divisions (see section 2.2.2 and Table 1), proving that the P values calculated (Figure 2) as if the SOI data are serially independent, are consequential. Although higher order polynomial regressions may result in lower MAE values [Pool, 2005], they can also result in a larger error for a single prediction; therefore, decision makers need to decide whether to use higher order polynomials for predictive regression models.

[32] Improvements in dichotomous predictions of higher or lower than mean winter precipitation relative to the trivial predictor (always lower than the mean) are significant in the same climate divisions where SOI and precipitation are highly correlated ($r < -0.45$, Table 1). The advantage of logistic regression is that it provides the probability for higher than average precipitation. Therefore, percentage of successful predictions for high or low probabilities ($\text{Pr} > 0.6$ or $\text{Pr} < 0.4$) which occurred over a certain percentage of time for the climate divisions (AZ4, 46%; CA7, 68%; OK8, 70%; FL3, 73%; TX8, 74%; and NE2, 77%) is higher than those made for the complete set of predictions ($\text{Pr} \geq 0.5$ or $\text{Pr} < 0.5$; Table 1). For example, successful predictions increased by 14% (relative to trivial predictions) in OK8 and AZ4 when using the higher or lower probabilities alone (Table 1), suggesting that use of logistic regression models is worthwhile also in areas of lower SOI-precipitation correlation and the high PDO area in the south central region. The success rate in these high and low probability cases was $\geq 75\%$ in climate divisions where SOI and precipitation are highly correlated (TX8, FL3, and NE2, Table 1).

[33] Predicting whether winter precipitation would be in the three higher quartiles using SOI and PDO-phase data was improved relative to the trivial prediction (always in the three higher quartiles –75% success) only in TX8 and OK8 where the PDO phase and La Niña conditions have a stronger impact on precipitation (Table 1).

[34] Summarizing this prediction-validation analysis, substantial increases in predictability of winter precipitation

over trivial predictions with June⁰-September⁰ SOI and PDO-phase data can be obtained in areas where the correlation coefficient between historic SOI and precipitation data is < -0.45 . This area includes the three southern climate divisions in Arizona, almost all the coastal climate divisions on the Gulf of Mexico, and climate divisions 2 and 7 in Nebraska (in red in Figure 8b). In other climate divisions where a significant correlation exists between historic SOI and precipitation data ($\sim r < -0.2$ in the 100 a data set), improvement in predictions is relatively minor. Nevertheless, high or low probabilities obtained by logistic regression models gave above/below mean-precipitation predictions in the 70% success level also in regions where $r \geq -0.4$. The percentage of successful predictions obtained in this analysis does not show the full strength of logistic regression models because it does not use the exact probabilities calculated by the models. These probabilities can be very helpful for calculating expected values of precipitation-related variables (e.g., agricultural yield and income from a precipitation-related economic activity). The PDO phase improved precipitation prediction only in TX8 and OK8 climate divisions. Whereas SOI is always known at the beginning of a hydrologic year, the PDO phase is often debatable. Nevertheless, non-ENSO cold phase years are expected to have lower than average winter precipitation in the Texas-Oklahoma area. For example, the probabilities based on the logistic regression models for 2005–2006 October⁰-March⁺ precipitation, which followed a non-ENSO summer (SOI = 0.01), assuming cold-phase PDO, were $\text{Pr} = 0.29$ and $\text{Pr} = 0.36$ for above mean precipitation in climate divisions OK8 and TX8, respectively. October-March precipitation in both climate divisions was far below average in 2005–2006.

4. Conclusions

[35] A continuous, statistically significant ($P < 0.05$), wet-El-Nino and dry-La-Nina winter (October-March) region was found in response to ENSO (June-September SOI) forcing, extending from North Carolina in the east to southern California in the west and as far north as South Dakota in the center, based on analysis of climate division precipitation data from 1905–2005 in the southern United States. Centers of highest correlation were found along the Gulf of Mexico, southern Arizona, and a previously ignored

area centered in Nebraska. Similar results were found for analysis of annual precipitation; however, correlations are weaker and the area affected is smaller for annual than for winter precipitation.

[36] The strength and spatial distribution of ENSO-related precipitation anomalies in the southern United States vary with the extremity of composites used to calculate the anomaly (e.g., upper decile or upper quartile SOI) and whether relative or absolute anomalies are considered. Highest relative anomalies are found in Arizona, New Mexico, and Nebraska when the less extreme composite (upper quartile) was used, while the entire southwest is the most affected region when the more extreme composite (upper decile) was used. Absolute anomalies were greatest along the Gulf of Mexico and Texas.

[37] Pacific Decadal Oscillation impacts on winter precipitation are significant ($P < 0.1$) only in the south central region (New Mexico to Louisiana), with highest significance in Oklahoma. Climate divisions in which the 50% PDO anomaly is greater than the 50% SOI anomaly are primarily in Oklahoma, Arkansas, and Missouri, which are outside the areas that have high correlations between SOI and precipitation. Decadal modulation of El Niño (higher anomalies during PDO warm phase) was found in the southeast (Louisiana to Florida) and southwest (Arizona, Utah, Nevada, and California) while decadal modulation of La Niña was found in the north-central region (Kansas to South Dakota). In the south central region (Texas and Oklahoma) both El Niño and La Niña decadal modulations exist and the latter is stronger.

[38] Testing of winter precipitation prediction models in a representative set of climate divisions (6) relative to trivial predictors (precipitation mean and median) indicated that summer SOI was a useful predictor of winter precipitation in all six climate divisions. PDO-phase was useful only in the two south central climate division regions tested in Texas and Oklahoma. The decrease in relative mean absolute error (MAE) over the MAE of a trivial prediction (mean precipitation) was greatest (9%–16%) in three out of the six climate divisions in which the correlation coefficient between SOI and winter precipitation is relatively strong ($r < -0.45$).

[39] A novel application of logistic regression models that use summer-SOI and PDO phase data for calculating the probability of exceeding the mean winter precipitation was found to improve the success over trivial predictions (always below the mean) by 14%–18% in climate divisions where SOI and precipitation are strongly correlated ($r < -0.45$). Increases in prediction success by up to 14% higher than the trivial predictor when only the higher and lower probabilities ($Pr > 0.6$ and $Pr < 0.4$) were considered, was found also in climate divisions with low correlation between SOI and precipitation ($r \geq -0.40$), suggesting that use of probabilities calculated from SOI and/or PDO-phase logistic models could be beneficial over large areas. The advantage of having probabilities of exceeding a pre-specified precipitation threshold at the beginning of a hydrologic year can be highly beneficial to water resource managers.

[40] **Acknowledgments.** This research was supported by the Jackson School of Geosciences, University of Texas at Austin. The authors would like to thank Hugo Hidalgo (UC-San Diego), Huade Guan (UT-San

Antonio), Harry Lins (USGS), Ian Ferguson (UC-Berkeley), and three anonymous reviewers for their helpful reviews of the manuscript. The first author would also like to thank the staff and associates of the Reservoir Characterization Research Laboratory (RCRL) at the Bureau of Economic Geology, University of Texas at Austin, for providing time to finalize this paper.

References

- Andrade, E. R., and W. D. Sellers (1988), El Niño and its effect on precipitation in Arizona and western New Mexico, *J. Climatol.*, *8*, 403–410.
- Bond, N. A., J. E. Overland, M. Spillane, and P. Stabeno (2003), Recent shifts in the state of the North Pacific, *Geophys. Res. Lett.*, *30*(23), 2183, doi:10.1029/2003GL018597.
- Brown, D. P., and A. C. Comrie (2004), A winter precipitation “dipole” in the western United States associated with multidecadal ENSO variability, *Geophys. Res. Lett.*, *31*, L09203, doi:10.1029/2003GL018726.
- Chen, C. C., D. Gillig, B. A. McCarl, and R. L. Williams (2005), ENSO impacts on regional water management: Case study of the Edwards Aquifer (Texas, USA), *Clim. Res.*, *28*, 175–181.
- CIMSS (2006), A cooperative institute formed through a memorandum of understanding between the University of Wisconsin-Madison (UW-Madison), the National Oceanic and Atmospheric Administration (NOAA), and the National Aeronautics and Space Administration (NASA): CIMSS scientists conduct research using passive remote sensing systems for meteorological and surface-based applications, Univ. of Wis., Madison.
- Dettinger, M. D., D. R. Cayan, H. F. Diaz, and D. M. Meko (1998), North-south precipitation patterns in western North America on interannual-to-decadal timescales, *J. Clim.*, *11*, 3095–3111.
- Dracup, J. A., and E. Kahya (1994), The relationships between United States streamflow and La Niña events, *Water Resour. Res.*, *30*, 2133–2141.
- Eichler, E., and W. Higgins (2006), Climatology and ENSO-related variability North American extratropical cyclone activity, *J. Clim.*, *19*, 2076–2093.
- Gershunov, A., and T. P. Barnett (1998), Interdecadal modulation of ENSO teleconnections, *Bull. Am. Meteorol. Soc.*, *79*, 2715–2725.
- Goodrich, G. B. (2004), Influence of the Pacific decadal oscillation on Arizona winter precipitation during years of neutral ENSO, *Weather Forecasting*, *19*, 950–953.
- Grimm, A. M., S. E. T. Ferraz, and J. Gomes (1998), Precipitation anomalies in southern Brazil associated with El Niño and La Niña events, *J. Clim.*, *11*, 2863–2880.
- Guan, H., E. R. Vivoni, and J. L. Wilson (2005), Effects of atmospheric teleconnections on seasonal precipitation in mountainous regions of the southwestern U. S.: A case study in northern New Mexico, *Geophys. Res. Lett.*, *32*, L23701, doi:10.1029/2005GL023759.
- Guttman, N., and R. G. Quayle (1996), A historical perspective of U.S. climate divisions, *Bull. Am. Meteorol. Soc.*, *77*, 293–303.
- Gutzler, D. S., D. M. Kann, and C. Thornbrugh (2002), Modulation of ENSO-based long-lead outlooks of southwestern US winter precipitation by the Pacific decadal oscillation, *Weather Forecasting*, *17*, 1163–1172.
- Hanley, D. E., M. A. Bourassa, J. J. O’Brien, S. R. Smith, and E. R. Spade (2003), A quantitative evaluation of ENSO indices, *J. Clim.*, *16*, 1249–1258.
- Hanson, R. T., M. W. Newhouse, and M. D. Dettinger (2004), A methodology to assess relations between climatic variability and variations in hydrologic time series in the southwestern United States, *J. Hydrol.*, *287*, 252–269.
- Hidalgo, H. G., and J. A. Dracup (2003), ENSO and PDO effects on hydroclimatic variations of the Upper Colorado River basin, *J. Hydro-meteorol.*, *4*, 5–23.
- Kahya, E., and J. A. Dracup (1993), United States streamflow patterns in relation to the El Niño–Southern Oscillation, *Water Resour. Res.*, *29*, 2491–2503.
- Kiladis, G. N., and H. F. Diaz (1989), Global climate anomalies associated with extremes of the Southern Oscillation, *J. Clim.*, *2*, 1069–1090.
- Mantua, N. J., S. R. Hare, Y. Zhang, J. M. Wallace, and R. C. Francis (1997), A Pacific interdecadal climate oscillation with impacts on salmon production, *Bull. Am. Meteorol. Soc.*, *78*, 1069–1079.
- McCabe, G. J., and M. D. Dettinger (1999), Decadal variation in the strength of ENSO teleconnections with precipitation in the western United States, *Int. J. Climatol.*, *19*, 1399–1410.
- McPhaden, M. J., S. E. Zebiak, and M. H. Glantz (2006), ENSO as an integrating concept in Earth science, *Science*, *314*, 1740–1745.

- Newman, M., G. P. Compo, and M. A. Alexander (2003), ENSO-forced variability of the Pacific decadal oscillation, *J. Clim.*, *16*, 3853–3857.
- Noel, J., and D. Changnon (1998), A pilot study examining US winter cyclone frequency patterns associated with three ENSO parameters, *J. Clim.*, *11*, 2152–2159.
- Peterson, W. T., and F. B. Schwing (2003), A new climate regime in northeast Pacific ecosystems, *Geophys. Res. Lett.*, *30*(17), 1896, doi:10.1029/2003GL017528.
- Piechota, T. C., and J. A. Dracup (1996), Drought and regional hydrologic variation in the United States: Associations with the El Niño–Southern Oscillation, *Water Resour. Res.*, *32*, 1359–1373.
- Pool, D. R. (2005), Variations in climate and ephemeral channel recharge in southeastern Arizona, United States, *Water Resour. Res.*, *41*, W11403, doi:10.1029/2004WR003255.
- Rasmusson, E. M., and T. H. Carpenter (1982), Variations in tropical sea surface temperature and surface wind fields associated with the Southern Oscillation/El Niño, *Mon. Weather Rev.*, *110*, 354–384.
- Redmond, K. T., and R. W. Koch (1991), Surface climate and streamflow variability in the western United States and their relationship to large-scale circulation indexes, *Water Resour. Res.*, *27*, 2381–2399.
- Ropelewski, C. F., and M. S. Halpert (1986), North American precipitation and temperature patterns associated with the El Niño–Southern Oscillation (ENSO), *Mon. Weather Rev.*, *114*, 2352–2362.
- Ropelewski, C. F., and M. S. Halpert (1987), Global and regional precipitation patterns associated with El-Niño–Southern Oscillation, *Mon. Weather Rev.*, *115*, 1606–1626.
- SAS Institute Inc. (2004), SAS/STAT 9.1 user's guide, Cary, N. C. (Available at http://support.sas.com/documentation/onlinedoc/91pdf/sasdoc_91/stat_ug_7313.pdf)
- Simpson, H. J., and D. C. Colodner (1999), Arizona precipitation response to the Southern Oscillation: A potential water management tool, *Water Resour. Res.*, *35*, 3761–3769.
- Sun, H. B., and D. J. Furbish (1997), Annual precipitation and river discharges in Florida in response to El Niño and La Niña sea surface temperature anomalies, *J. Hydrol.*, *199*, 74–87.
- Trenberth, K. E. (1997), The definition of El Niño, *Bull. Am. Meteorol. Soc.*, *78*, 2771–2777.
- Trenberth, K. E., G. W. Branstator, D. Karoly, A. Kumar, N. C. Lau, and C. Ropelewski (1998), Progress during TOGA in understanding and modeling global teleconnections associated with tropical sea surface temperatures, *J. Geophys. Res.*, *103*, 14,291–14,324.
- Wolter, K., and M. S. Timlin (1993), Monitoring ENSO in COADS with a seasonally adjusted principal component index, paper presented at 17th Climate Diagnostics Workshop, Univ. of Okla., Norman.

D. Kurtzman, Department of Environmental Health Sciences, Hadassah College, Hanevi'im 37, P.O. Box 114, Jerusalem 91010, Israel. (zkj2007@012.net.il)

B. R. Scanlon, Bureau of Economic Geology, Jackson School of Geosciences, University of Texas at Austin, 10100 Burnet Road, Austin, TX 78758, USA. (bridget.scanlon@beg.utexas.edu)